

Local Measurements of Magnetization in Mn_{12} Crystals

Nurit Avraham,^{1,2} Ady Stern,¹ Yoko Suzuki,² K. M. Mertes,² M. P. Sarachik,² E. Zeldov,¹ Y. Myasoedov,¹ H. Shtrikman,¹ E. M. Rumberger,³ D. N. Hendrickson,³ N. E. Chakov,⁴ and G. Christou⁴

¹*Dept. of Condensed Matter Physics, The Weizmann Institute of Science, Rehovot 76100, Israel*

²*Physics Department, City College of the City University of New York, New York, NY 10031*

³*Dept. of Chemistry and Biochemistry, University of California at San Diego, La Jolla, CA 92093*

⁴*Department of Chemistry, University of Florida, Gainesville, FL 32611*

(Dated: March 23, 2022)

The spatial profile of the magnetization of Mn_{12} crystals in a swept magnetic field applied along the easy axis is determined from measurements of the local magnetic induction along the sample surface using an array of Hall sensors. We find that the magnetization is not uniform inside the sample, but rather shows some spatial oscillations which become more prominent around the resonance field values. Moreover, it appears that different regions of the sample are at resonance at different values of the applied field and that the sweep rate of the internal magnetic induction is spatially non-uniform. We present a model which describes the evolution of the non-uniformities as a function of the applied field. Finally we show that the degree of non-uniformity can be manipulated by sweeping the magnetic field back and forth through part of the resonance.

Molecular magnets, or single molecule magnets, are typically composed of magnetic cores surrounded by organic complexes. With a total spin of $S = 10$ and strong easy axis anisotropy^{1,2,3,4,5,6,7,8}, $[\text{Mn}_{12}\text{O}_{12}(\text{CH}_3\text{COO})_{16}(\text{H}_2\text{O})_4] \cdot 2\text{CH}_3\text{COOH} \cdot 4\text{H}_2\text{O}$ (generally referred to as Mn_{12} -acetate) has received a great deal of attention. When crystallized, Mn_{12} forms a tetragonal lattice⁹ with the easy magnetization direction along the c-axis. The magnetic cores are well separated⁹, so that exchange interactions between the molecules are negligible^{5,6,7,10}. The main terms in the spin Hamiltonian of Mn_{12} are given by

$$H = -DS_z^2 - g_z\mu_B B_z S_z - AS_z^4$$

The first term is the magnetic anisotropy energy, with $D = 0.548(3)\text{K}$ while the third term represents the next higher-order term in longitudinal anisotropy, with $A = 1.173(4) \times 10^{-3}\text{K}$ ^{11,12,13}. The second term is the Zeeman coupling to a magnetic field B_z along the easy-axis. In the absence of a magnetic field, this Hamiltonian can be represented as a symmetric double well potential with a set of energy levels corresponding to the $(2S+1) = 21$ allowed values of the quantum number S_z . A magnetic field B_z lifts the degeneracy of $\pm S_z$ states on opposite sides of the potential barrier, and a strong field B_z causes most of the molecules to occupy states in one of the wells. When B_z is swept, e.g., from positive to negative values, molecules relax from one side of the potential barrier to the other either via thermal activation over the barrier or by quantum tunneling through the barrier. Measurements below the blocking temperature of 3K show resonant tunneling of the magnetization, manifested as a series of step steps in the hysteresis loop at roughly equal intervals of magnetic field^{14,15,16,17}. The steps occur at magnetic field values where states on opposite sides of the barrier have the same energy, and are at “resonance”.

One of the common experimental techniques to study the tunneling of the magnetization is to measure the mag-

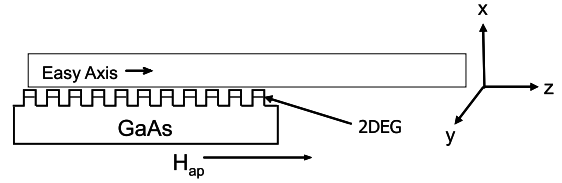


FIG. 1: Schematic diagram of the experimental setup. The Mn_{12} crystal, with a typical size of $z = 400 \mu\text{m}$, $y = 100 \mu\text{m}$ and $x = 40 \mu\text{m}$ is placed directly on the surface of an array of $10 \times 10 \mu\text{m}^2$ sensors that are $10 \mu\text{m}$ apart. The sensors cover only half the sample and measure the perpendicular component (B_x) of the magnetic induction at the surface.

netic response of the crystal when an external magnetic field H_a is applied parallel to the easy axis, and is swept through a series of resonances along the hysteresis loop. To date, studies of extended samples have provided the magnetic induction (and its variation in a swept magnetic field) as averages over the whole sample, or they have assumed that values measured in a limited region of space represent the average. As such, these measurements do not provide any information on the spatial profile of the magnetization in the sample, or on how the relaxation process propagates spatially within the sample.

The experiment reported here utilizes an array of sensors to measure the spatial variation of the magnetization in a Mn_{12} crystal as H_a is swept. Within our model we find the magnetization to be significantly non-uniform along the sample, with the non-uniformity being enhanced within the steps. Furthermore, it appears that different regions of the sample are at resonance at different values of the applied field, and that the sweep rate of the internal magnetic induction is spatially non-uniform. We demonstrate that the degree of non-uniformity can be manipulated by sweeping the magnetic field back and forth through part of the resonance.

The local induction of single Mn_{12} crystals of typical

size $400 \times 100 \times 40 \mu\text{m}^3$ was measured using an array of eleven Hall sensors¹⁸. The active layer of these sensors is a two dimensional electron gas formed at the interface of GaAs/AlGaAs heterostructure. The samples were mounted onto the surface of an array of $10 \times 10 \mu\text{m}^2$ sensors that were $10 \mu\text{m}$ apart, with the easy-axis parallel to the z -direction and to the applied field H_a , as shown in Fig. 1. The eleven sensors measure B_x , the x -component of the magnetic induction due to the magnetization of the crystal. Since the two dimensional electron gas resides only $0.1 \mu\text{m}$ below the surface, the induction measured by the sensors is practically equal to the induction at the crystal surface. As shown in Fig. 1, the center of the crystal was aligned with the array so that ten sensors probed the field along half the crystal length and the last sensor measured the field at the edge of the sample.

Fig. 2a and 2b show two local hysteresis loops of $B_x(H_a)$, at $T = 0.3\text{K}$, measured simultaneously at the edge of the sample and close to its center. The curves were obtained starting from a fully magnetized state by sweeping H_a from -6T up to 6T and back. The loop measured locally at the edge of the sample (Fig. 2a) resembles previously measured magnetization loops. When increasing H_a from zero to 6T , B_x increases monotonically toward its positive saturation value while displaying a series of steep steps at roughly equal intervals of magnetic field, due to resonant tunneling of the magnetization.

In contrast, the magnetic induction measured close to the center of the sample (shown in Fig. 2b) displays non-monotonic behavior as a function of H_a . The resonances are not manifested by a series of steps, but rather by a series of peaks and dips whose width is larger than that of the steps in Fig. 2a. Similar behavior is observed at other sensors located between the edge and the center of the sample. In general, B_x is largest close to the edge and decreases towards the center of the sample. The non-monotonic dependence on H_a , however, is most pronounced close to the center and gradually diminishes when proceeding towards the edge of the sample. The remarkable difference in the dependence of B_x on H_a observed by the different sensors contradict the assumption that the magnetization is uniform inside the sample. In general¹⁹, $B_x(\vec{r}, H_a) = \int d\vec{r}' M(\vec{r}', H_a) f(\vec{r} - \vec{r}')$, where $M(\vec{r}', H_a)$ is the magnetization at point \vec{r}' , that is assumed to be parallel to the easy axis, and

$$f(\vec{r} - \vec{r}') = -\frac{3(z - z')(x - x')}{|r - r'|^5}$$

If $M = M_0(H_a)$ is independent of \vec{r}' , we get $B_x(\vec{r}, H_a) = M_0(H_a) \int d\vec{r}' f(\vec{r} - \vec{r}')$, so that the $B_x(H_a)$ curves measured by all sensors should collapse onto a single curve when multiplied by a scaling factor. As the inner curves are non-monotonic while the edge curves are monotonic, this scaling cannot be realized, and the magnetization is therefore non-uniform.

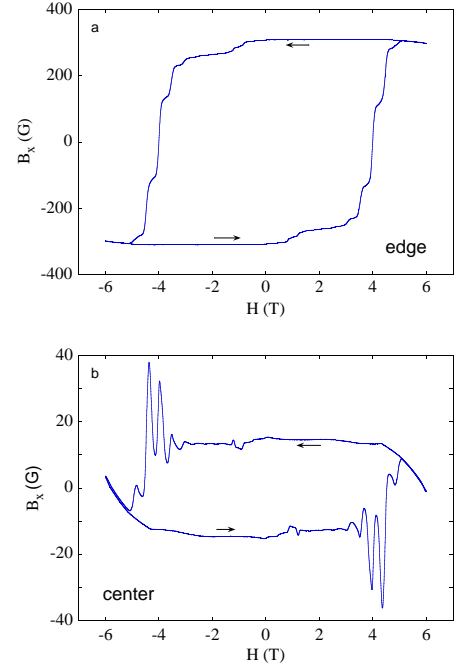


FIG. 2: Local hysteresis loops of B_x as a function of H_a ($T = 0.3\text{K}$), measured simultaneously at two different positions on the sample: (a) close to the edge and, (b) close to the center of the sample.

The non-uniformity of the magnetization is the source of the non-monotonicity displayed in Fig. 2b. Spins pointing in the same direction that are located on opposite sides of a sensor make *opposite* contributions to B_x . Due to these opposite contributions, the magnetic induction B_x measured by a sensor located close to the center of the sample is very small when all the spins in its surrounding point in the same direction, but is enhanced when the magnetization on the two sides is different. This enhancement may bring B_x to a value larger than its value when the sample becomes fully magnetized, as shown in Fig. 2b. Now, if the relaxation rates on the two sides of the sensor are different, the non-uniformity in the magnetization varies, and so does B_x . The direction in which B_x varies with H_a indicates the relative magnitudes of the relaxation rates on the two sides of the sensor. The situation is different for a sensor located near the edge of the sample, where all spins are on one side, and therefore their contributions to B_x add. For this sensor, inhomogeneities in the magnetization only broaden the steps, but do not result in non-monotonic behavior. This qualitative picture is further discussed below in terms of an equation for the time evolution of the local magnetization.

We now proceed to extract the spatial profile of the magnetization from the profile $B_x(z)$ measured by the sensors. Assuming that the sample has a perfect rectangular shape, and the magnetization is uniform along the

x and y directions, the induction B_x can be written as

$$B_x(z) = - \int dz' F(z-z') \frac{\partial M(z')}{\partial z} \quad (1)$$

where

$$F(z-z') = \log \frac{w_1 + \sqrt{w_1^2 + d_1^2 + (z-z')^2}}{w_1 + \sqrt{w_1^2 + d_2^2 + (z-z')^2}} - \log \frac{w_2 + \sqrt{w_2^2 + d_1^2 + (z-z')^2}}{w_2 + \sqrt{w_2^2 + d_2^2 + (z-z')^2}} \quad (2)$$

For the samples we used, $d_1 = 0.1 \mu\text{m}$ is the distance in the x direction between the sample surface and the 2DEG, $d_2 = 40 \mu\text{m}$ is the distance between the 2DEG and the sample's other surface, and $w_1 = -5 \mu\text{m}$, $w_2 = 85 \mu\text{m}$ are the distances between the center of the sensors and the edges of the sample in the y -direction.

$F(z-z')$ is a short-range function, whose characteristic decay length is typically $10 \mu\text{m}$ for our geometry. Eq. (1) implies that the magnetic field B_x measured by a sensor on the sample surface is proportional to the derivative $\frac{\partial M}{\partial z}$ in the vicinity of the sensor, and therefore Figs. 2a and 2b approximate the dependence of $\frac{\partial M}{\partial z}$ on H_a at the edge of the sample and close to the center of the sample, respectively.

Assuming that the magnetization varies smoothly over the scale of our sensors, we interpolate the measured $B_x(z)$ and numerically invert the kernel $F(z-z')$ to extract the magnetization profile $M(z, H_a)$. Figure 3 shows the resulting magnetization as a function of position for various values of H_a . Since our sensors cover only half the sample, we rely on the (nearly) symmetric shape of the samples and assume the magnetization to be symmetric with respect to the sample center. The non-uniformity of the magnetization and its evolution as a function of H_a are clearly demonstrated. Focusing first on the central part of the sample, we note that at -5.7T , where the sample is presumably fully magnetized, the magnetization is approximately uniform. When increasing the field to 3.6T the magnetization starts to develop a small amount of non-uniformity, manifested by the small variations of the magnetization from the average value. These variations continue to develop and become more pronounced at 3.9T , when the magnetization in most of the sample shows a high relaxation rate. The non-uniformities then decay somewhat at 4.14T , where the sample is out of resonance, and become prominent once more at the next resonance, at 4.3T . When increasing the field further to 5.7T the non-uniformities disappear and the magnetization becomes uniform again. Non-uniformities similar to those presented in Fig. 3 were observed in several samples, where they are enhanced when most of the sample is at resonance, and become minor away from resonances.

At the very edge of the sample the magnetization is expected to change abruptly from zero outside the sample to a non-zero value inside the sample. We believe that the gradual variation observed at all field values results from two major sources. First, the field B_x at the

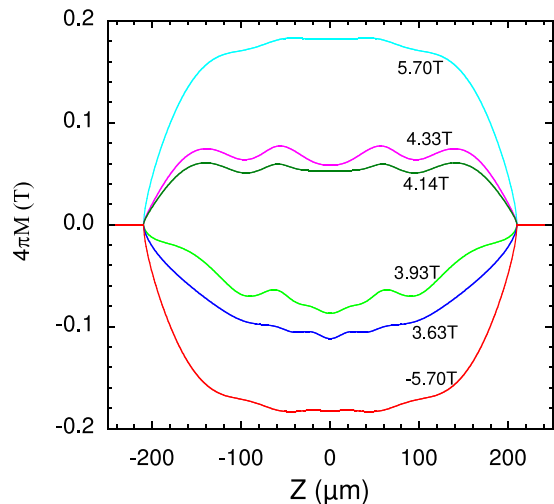


FIG. 3: The calculated profile of the magnetization plotted as a function of the distance from the center of the sample, at six different values of the applied field. Note the enhanced non-uniformity at fields close to resonances, at 3.9T and 4.33T .

edge of the sample varies significantly over the length of one sensor, and therefore the average field measured by the edge sensor may deviate appreciably from its local value. Second, the calculation of the magnetization is carried out assuming the sample has a perfect rectangular shape. Deviations from this shape, for example edges that are not perpendicular to the plane of the sensors, could also contribute to the rounding of the data at the edges. Note, however, that these effects cannot introduce the observed non-uniformities in the center of the sample. We also note that the overall scale of the magnetization obtained from our calculation is not very different from that expected: at full magnetization, $4\pi M$ is 0.12T for Mn_{12} crystals, while the maximum value shown in Fig. 3 is 0.18T .

The non-uniformity of the magnetization implies that B_z , the internal magnetic field in the z direction, is spatially non-uniform. Consequently, different parts of the sample enter the resonance at different values of H_a . We will now demonstrate that the internal sweep rate $\frac{\partial B_z}{\partial t}$ is spatially non-uniform as well, so that different parts of the sample spend different times at resonance. Under the assumption used to extract $M(z)$, B_z inside the sample can be written as

$$B_z(z) = H_a + 4\pi M(z) + \int dr' \frac{\partial M(r')}{\partial z'} \frac{z-z'}{|r-r'|^3} \quad (3)$$

Since all the terms and their time dependence are available from our analysis, we can directly derive the local sweep rate $\frac{\partial B_z}{\partial t}$.

This is shown in Fig. 4 as a function of position in the central part of the sample for different values of H_a . Two major observations are of particular interest. The first is that at 3.9T and at 4.3T , when the sample is at resonance, the internal sweep rate is much higher than

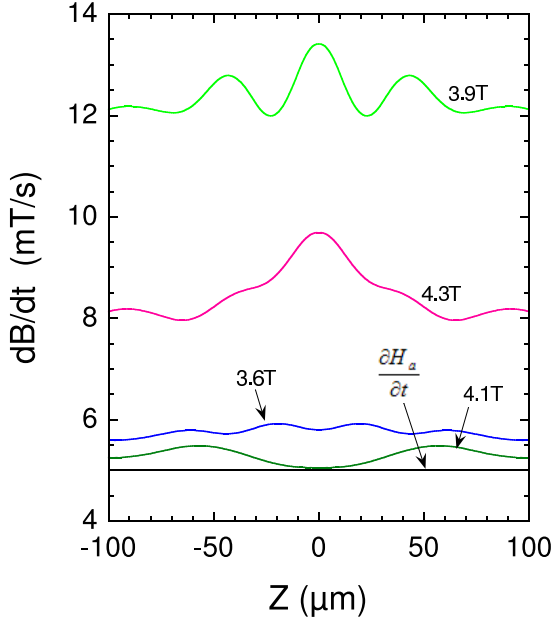


FIG. 4: Calculated sweep rate of the internal field, $\frac{\partial B_z}{\partial t}$, plotted as a function of the distance from the center of the sample, for the same field values as in Fig. 3. Note that when most of the sample is at resonance, at 3.9T and 4.3T, the internal sweep rate $\frac{\partial B_z}{\partial t}$ is much higher than the external sweep rate, $\frac{\partial H_a}{\partial t}$. Moreover, at these fields $\frac{\partial B_z}{\partial t}$ is significantly non-uniform inside the sample. When the sample is out of resonance, at 3.6T and 4.1T, the internal sweep rate is approximately uniform inside the sample and is very close to the sweep rate of the external field.

the nominal sweep rate of the external field. For example, $\frac{\partial B_z}{\partial t}$ is about 2.5 times larger than $\frac{\partial H_a}{\partial t}$ at 3.9T. In contrast, at 3.6T and 4.1T, when the sample is out of resonance, the sweep rates of B_z and H_a are approximately equal. The second major observation is that at resonance fields, $\frac{\partial B_z}{\partial t}$ is highly non-uniform and can vary by as much as 20% over a distance of the order of 50 μm . This means not only that different regions enter the resonance at different H_a , but also that the times spent by local regions at resonance can be significantly different.

As we show below, the observed spatial non-uniformities and their evolution with H_a can be explained by a simple model describing the relaxation of the magnetization along the hysteresis loop. Initially, at 6T, the magnetization is uniform inside the sample. However the relaxation rate is non-uniform due to the spatial variation of the internal magnetic field and due to molecular and structural disorder. Therefore, as we sweep the magnetic field to -6T (in the opposite direction) non-uniformity in the magnetization begins to develop. Under certain conditions, and particularly within resonances, the non-uniformity in the magnetization grows with time, despite the decay in the magnetization itself. The magnetization is non-uniform even when the sample is out of resonance and the relaxation rates are negligible. We attribute the non-uniformity in the magnetization off resonance to the

spatial variation of the sweep rate (Fig. 4) that causes different regions of the sample to spend different times at resonance.

In our model the relaxation of the space- and time-dependent magnetization $M(z, t)$ is governed by the equation

$$\frac{\partial M}{\partial t} = -(M - M_0)\Gamma \quad (4)$$

where M_0 is the equilibrium magnetization and Γ is the relaxation rate, which near a resonance has a general form

$$\Gamma = \Gamma_0 \frac{\alpha^2}{(B_z - B_r)^2 + \alpha^2} \quad (5)$$

where B_r is the magnetic induction at the center of the resonance, and 2α is the resonance width. Molecular disorder introduces variations of Γ_0 , B_r and α between different molecules. However, since the distribution of these parameters does not depend on position, we use their average values. The non-uniformity of the magnetization is characterized by its spatial derivative $\frac{\partial M}{\partial z}$. We may use Eq. (4) to analyze the time evolution of $\frac{\partial M}{\partial z}$. To that end, we take the derivative of (4) with respect to z , and approximate $B(z) \approx H_a + 4\pi M(z)$ (i.e., we neglect the third term in Eq. (3), which is small in the central part of the sample). We obtain

$$\frac{\partial}{\partial t} \frac{\partial M}{\partial z} = -[\Gamma + 4\pi(M - M_0) \frac{\partial \Gamma}{\partial B}] \frac{\partial M}{\partial z} \quad (6)$$

Although the dependence of Γ on $M(z)$ makes this equation a non-linear differential equation, the conditions under which non-uniformities in the magnetization grow with time are rather transparent. The question of whether the magnitude of $\frac{\partial M}{\partial z}$ increases or decreases with time is determined by the balance between the two terms on the right hand side of this equation. The first term acts to suppress the magnitude of $\frac{\partial M}{\partial z}$, i.e., the magnitude of the non-uniformity. The effect of the second term, on the other hand, depends on the sign of $(M - M_0) \frac{\partial \Gamma}{\partial B}$. When this sign is negative, this term tends to enhance the magnitude of the non-uniformity. If strong enough, it may overcome the effect of the first term. When that happens, the magnetization $M(z)$ relaxes towards M_0 , but its non-uniformity $|\frac{\partial M}{\partial z}|$ increases with time.

From Eq. (6), it is easy to verify that as long as $|M - M_0| < \frac{\alpha}{4\pi}$,

$$\Gamma + 4\pi(M - M_0) \frac{\partial \Gamma}{\partial B} > 0 \quad (7)$$

for any B_z and hence the non-uniformity is suppressed with time. However, when $|M - M_0| > \frac{\alpha}{4\pi}$, there is a range of B_z

$$(M - M_0) - \sqrt{(M - M_0)^2 - \frac{\alpha^2}{(4\pi)^2}} < \frac{(B_z - B_r)}{4\pi} < (M - M_0) + \sqrt{(M - M_0)^2 - \frac{\alpha^2}{(4\pi)^2}} \quad (8)$$

at which $\Gamma + 4\pi(M - M_0)\frac{\partial\Gamma}{\partial B} < 0$ and the non-uniformity is enhanced with time. We consider, for concreteness, the case where H_a is swept down from 6T to -6T through one of the resonances. In this case M_0 is negative, and $M - M_0$ is positive. If $M - M_0 \gg \frac{\alpha}{4\pi}$, the range (8) occupies the first half of the resonance, where $B_z > B_r$. As H_a is swept down, the non-uniformity grows during the first half of the resonance while $B_z > B_r$, and then is suppressed again when B_z drops below B_r . Such behavior is indeed observed in Fig. 3. In general, non-uniformities are always enhanced on approaching resonance, reaching maximum close to resonance and then suppressed after the resonance. Our measurements show resonances whose half-widths are about 0.045T. However, the measured half-widths are larger than the intrinsic half-width α , due to the effects of molecular disorder and hyperfine fields. The non-uniformities are found experimentally to evolve at the resonances where $4\pi(M - M_0) > 0.06T$, consistent with the model above.

Eq. (5) and the discussion following it suggest that the non-uniformity in the magnetization may be enhanced if the applied field H_a is tuned to a value where $\Gamma + 4\pi(M - M_0)\frac{\partial\Gamma}{\partial B}$ is negative at least in some parts of the sample, and is kept there for some time²⁰. Our measurements show that this is indeed the case. To identify the proper value of H_a , we note again that B_x is proportional to $\frac{\partial M}{\partial z}$ and therefore the observed slope $\frac{\partial B_x}{\partial H_a}$ measures the local slope $\frac{\partial}{\partial z} \frac{\partial M}{\partial t}$. Thus, when H_a is swept back and forth over a region where both $\frac{\partial B_x}{\partial H_a}$ and B_x have the proper signs, this sweep results in an enhancement of the non-uniformity. Figure 5a shows the effect of such a back-and-forth sweep on the magnetic induction B_x measured by a sensor located close to the center of the sample. Two curves are presented: a reference curve in which H_a was swept between -6T and 6T at a constant sweep rate; and the 'back-and-forth sweep' (BF sweep) curve in which H_a was swept up from -6T to 3.9T and then was swept back and forth between 3.9T and 3.69T. The reference curve shows a dip at 3.9T, signifying resonant relaxation of the magnetization. The range of the back-and-forth sweep was chosen to cover only half of this dip, at which both $\frac{\partial B_x}{\partial H_a}$ and B_x were negative. During the back-and-forth sweep the magnetic induction $|B_x|$ at $H_a = 3.9T$ increased to a value 3.5 times larger than its corresponding value at the reference curve. The strong increase in $|B_x|$ above the saturation value signifies a strong enhancement of the non-uniformity inside the sample, since B_x is proportional to the local spatial derivative of the magnetization, $\frac{\partial M}{\partial z}$, in the vicinity of the sensor.

Figure 5b demonstrates the enhancement of the non-uniformity in the magnetization profile $M(z)$ by the BF sweep. The lowest curve shows the magnetization at 3.68T just before sweeping the field back and forth over part of the resonance. At this point some non-uniformity has already developed. The three other curves correspond to three different measurements in which BF sweeping was carried out with three different amplitudes.

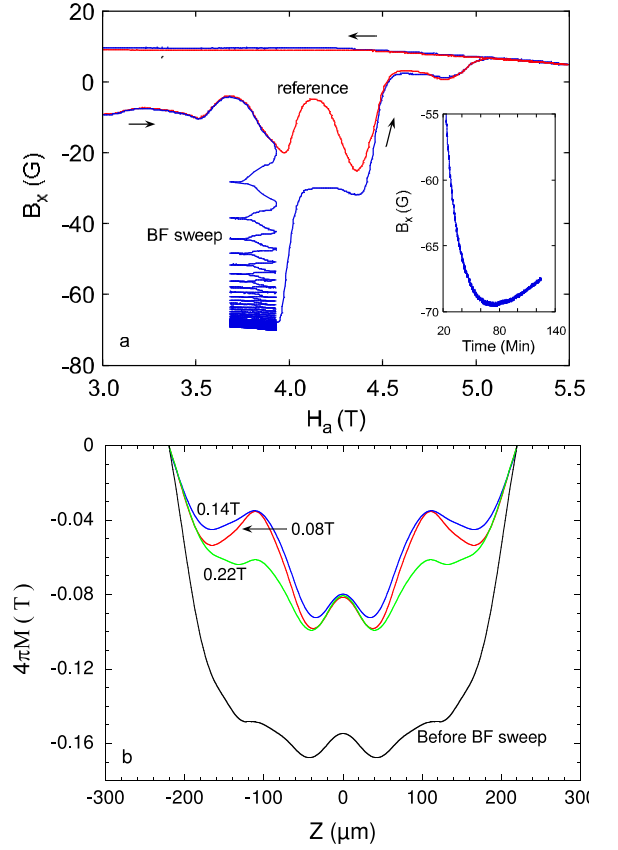


FIG. 5: Local hysteresis loops $B_x(H_a)$, measured close to the center of the sample. During the back and forth sweep the magnetic field B_x at $H_a = 3.9T$ decreases to -70G, which is 3.5 times larger than its corresponding value at the reference curve (-20G). The inset shows the evolution of B_x as a function of time during the BF sweep. (b) Magnetization profiles $M(z)$ showing the enhancement of the non-uniformity by the BF sweep. The lowest curve shows the magnetization at 3.68T before the BF sweep. The upper curves correspond to three different measurements in which the BF sweep was carried out with different amplitude of the BF cycle (0.08T, 0.14T, 0.22T)

In all measurements the cycle starts at the same field of 3.7T, and each measurement spans a different part of the transition. The most significant enhancement of the non-uniformity is displayed for the smallest amplitude of 0.08T, where the number of molecules that relaxed during the BF sweep strongly differs between the center and the edge of the sample. The effect is smaller for an amplitude of 0.14T, and yet smaller for an amplitude of 0.25T. While suggesting the possibility for magnetization non-uniformities that grow with time, Eqs. (5) and (6) also indicate that eventually, as relaxation progresses and the magnitude of $M - M_0$ gets smaller, $\Gamma + 4\pi(M - M_0)\frac{\partial\Gamma}{\partial B}$ must at some point become positive. Since $\frac{\partial M}{\partial z}$ is approximately proportional to the magnetic induction B_x measured by our sensors, this implies that when H_a is swept back and forth for long enough, the magnitude of

B_x must eventually decrease. This expectation is indeed borne out in the measurement. The inset of Fig. 5a presents the evolution of B_x during the back-and-forth sweeping as a function of time. The measured B_x initially increases in magnitude, but after about 70 minutes of sweeping, its magnitude starts to decrease. This change happens when the difference between the relaxation rates on both sides of the sensor changes sign. The source of this change in relaxation rates may be the decrease of the magnitude of $M - M_0$, or a change in the internal magnetic induction B_z that changes both Γ and $\frac{\partial \Gamma}{\partial B}$. We are presently unable to determine the relative weight of these two sources.

The saturation of the non-uniformity when $M - M_0$ becomes too small is plausibly also the source of the effect of the BF sweep on the following resonance. As shown in Fig. 5a, the BF sweeping of the field in the range between 3.69T and 3.9T changes the dip seen in the reference curve at 4.3T into a step. Within the framework of Eq. (5), the non-monotonic behavior of B_x around 4.3T, shown in the reference curve, signifies an enhancement of the non-uniformity followed by its suppression. In contrast, the almost monotonic step observed in the BF curve indicates that as a consequence of the back-

and-forth sweep, the resonance at 4.3T is traversed with $\Gamma + 4\pi(M - M_0)\frac{\partial \Gamma}{\partial B}$ remaining positive, such that no enhancement of the non-uniformity takes place.

To summarize, we used a set of Hall sensors to measure the local magnetic response of crystals of the molecular magnet Mn_{12} -acetate. Our measurements allowed us to determine the local magnetization in different regions of the crystal and its evolution as the crystal is driven through a hysteresis loop. We find significant non-uniformities, which are larger when resonant tunnelling takes place, but do not disappear when out of resonance. We explain how these non-uniformities result from the dipolar interaction between molecules. We show that the non-uniformity of the magnetization may be enhanced by sweeping the externally applied field back and forth through a properly chosen range. This method carries the potential for local manipulation of the magnetization profile inside the sample.

The work at City College of New York was supported by NSF grant DMR-0451605, and the work at WIS by the Israel Science Foundation Center of Excellence (grant No. 8003/02) and by the US-Israel Binational Science Foundation (BSF grants 2002238 and 2002242).

-
- ¹ A. Caneschi, D. Gatteschi, R. Sessoli, A. L. Barra, L. C. Brunel, and M. Guillot, *J. Am. Chem. Soc.* **113**, 5873 (1991).
 - ² R. Sessoli, H.-L. Tsai, A. R. Schake, S. Wang, J. B. Vincent, K. Folting, D. Gatteschi, G. Christou, and D. N. Hendrickson, *J. Am. Chem. Soc.* **115**, 1804 (1993).
 - ³ R. Sessoli, D. Gatteschi, A. Caneschi, and M. A. Novak, *Nature (London)* **365**, 141 (1993).
 - ⁴ R. Sessoli, *Mol. Cryst. Liq. Cryst.* **274**, A 145 (1995).
 - ⁵ M. A. Novak, R. Sessoli, A. Caneschi, and D. Gatteschi, *J. Magn. Magn. Mater.* **146**, 211 (1995).
 - ⁶ C. Paulsen and J.-G. Park, in *Quantum Tunneling of Magnetization*, edited by L. Guther and B. Barbara (Kluwer, Amsterdam/Dordrecht, 1995) (p. 189).
 - ⁷ M. A. Novak and R. Sessoli, in *Quantum Tunneling of Magnetization*, edited by L. Guther and B. Barbara (Kluwer, Amsterdam/Dordrecht, 1995) (p. 171).
 - ⁸ C. Paulsen, J.-G. Park, B. Barbara, R. Sessoli, and A. Caneschi, *J. Magn. Magn. Mater.* **140-144**, 1891 (1995).
 - ⁹ T. Lis, *Acta Crystallogr. Sec. B* **36**, 2042 (1980).
 - ¹⁰ C. Paulsen, J.-G. Park, B. Barbara, R. Sessoli, and A. Caneschi, *J. Magn. Magn. Mater.* **140-144**, 379 (1995).
 - ¹¹ A. L. Barra, D. Gatteschi, and R. Sessoli, *Phys. Rev. B* **56**, 8192 (1997).
 - ¹² S. Hill, J. A. A. J. Perenboom, N. S. Dalal, T. Hathaway, T. Stalcup, and J. S. Brooks, *Phys. Rev. Lett.* **80**, 2453 (1998).
 - ¹³ I. Mirebeau, M. Hennion, H. Casalta, H. Andres, H. U. Gudel, A. V. Irodova, and A. Caneschi, *Phys. Rev. Lett.* **83**, 628 (1999).
 - ¹⁴ J. R. Friedman, M. P. Sarachik, J. Tejada, J. Maciejewski, and R. Ziolo, *Jour. Appl. Phys.* **79**, 6031 (1996).
 - ¹⁵ J. R. Friedman, M. P. Sarachik, J. Tejada, and R. Ziolo, *Phys. Rev. Lett.* **76**, 3830 (1996).
 - ¹⁶ J. M. Hernandez, X. X. Zhang, F. Luis, J. Tejada, J. R. Friedman, M. P. Sarachik, and R. Ziolo, *Phys. Rev. B* **55**, 5858 (1997).
 - ¹⁷ L. Thomas, F. Lioni, R. Ballou, D. Gatteschi, R. Sessoli, and B. Barbara, *Nature* **383**, 145 (1996).
 - ¹⁸ E. Zeldov, D. Majer, M. Konczykowski, V. B. Geshkenbein, V. M. Vinokur, and H. Shtrikman, *Nature* **375**, 373 (1995).
 - ¹⁹ J. D. Jackson, *Classical Electrodynamics*, John Wiley and Sons, third edition (Eq. 5.56).
 - ²⁰ W. Wernsdorfer, T. Ohm, C. Sangregorio, R. Sessoli, D. Mailly, and C. Paulsen, *Phys. Rev. Lett.* **82**, 3903 (1999).